

Electronic Supplementary Information (*ESI*)

Microstructures of negative and positive azeotropes

J. J. Shephard,^{a, b} S. K. Callear,^c S. Imberti,^c J. S. O. Evans^b and C. G. Salzmann^{a*}

^a Department of Chemistry, University College London, 20 Gordon Street, WC1H 0AJ London, UK

^b Department of Chemistry, Durham University, South Road, Durham DH1 3LE, UK

^c ISIS Facility, Rutherford Appleton Laboratory, Didcot OX11 0QX, UK

* Corresponding author: c.salzmann@ucl.ac.uk (C. G. Salzmann)

Table of contents

1	Materials	2
2	Neutron scattering experiments	2
3	Empirical Potential Structural Refinement	3
4	Classification of local environments in the EPSR models	8
5	X-ray diffraction and differential scanning calorimetry upon cooling	9
6	Calculation of Kirkwood-Buff integrals from thermodynamic data	10
7	References	19

1 Materials

Acetone (CH_3COCH_3 and CD_3COCD_3), chloroform (CHCl_3 and CDCl_3), methanol (CH_3OH , CD_3OH and CD_3OD) and benzene (C_6D_6 and C_6H_6) were purchased from Sigma Aldrich, and used without further purification. Their quoted purities are >99.9 weight% and >99.96 D / H atom%. The various liquid mixtures were prepared by weighing the components into the same flasks and carefully mixed by inverting the flasks. The mole fractions of the azeotropes are $x_A=0.405$ and $x_M=0.550$ at 25°C .¹⁻³

The isotopic compositions of the various acetone-chloroform mixtures together with the scattering length density contrasts were:

- (1) 20.25 mol% CH_3COCH_3 , 20.25 mol% CD_3COCD_3 , 29.75 mol % CDCl_3 , 29.75 mol% CHCl_3 ($7.00 \times 10^{-9} \text{ \AA}^{-2}$)
- (2) 20.25 mol% CH_3COCH_3 , 20.25 mol% CD_3COCD_3 , 59.5 mol% CDCl_3 ($4.81 \times 10^{-8} \text{ \AA}^{-2}$)
- (3) 40.5 mol% CD_3COCD_3 , 59.5 mol% CDCl_3 ($2.08 \times 10^{-7} \text{ \AA}^{-2}$)
- (4) 40.5 mol% CH_3COCH_3 , 59.5 mol% CHCl_3 ($2.22 \times 10^{-7} \text{ \AA}^{-2}$)
- (5) 40.5 mol% CD_3COCD_3 , 29.75 mol% CDCl_3 , 29.75 mol% CHCl_3 ($2.49 \times 10^{-7} \text{ \AA}^{-2}$)
- (6) 40.5 mol% CD_3COCD_3 , 59.5 mol% CHCl_3 ($2.90 \times 10^{-7} \text{ \AA}^{-2}$)
- (7) 40.5 mol% CH_3COCH_3 , 59.5 mol% CDCl_3 ($3.04 \times 10^{-7} \text{ \AA}^{-2}$)

The isotopic compositions of the various benzene-methanol mixtures together with the scattering length density contrasts were:

- (1) 45 mol% C_6D_6 , 55 mol% CD_3OD ($3.70 \times 10^{-7} \text{ \AA}^{-2}$)
- (2) 45 mol% C_6D_6 , 27.5 mol% CD_3OH , 27.5 mol% CD_3OD ($3.92 \times 10^{-7} \text{ \AA}^{-2}$)
- (3) 22.5 mol% C_6D_6 , 22.5 mol% C_6H_6 , 27.5 mol% CD_3OD , 27.5 mol% CH_3OH ($5.76 \times 10^{-7} \text{ \AA}^{-2}$)
- (4) 45 mol% C_6D_6 , 55 mol% CD_3OH ($1.16 \times 10^{-6} \text{ \AA}^{-2}$)
- (5) 45 mol% C_6H_6 , 55 mol% CH_3OH ($1.55 \times 10^{-6} \text{ \AA}^{-2}$)
- (6) 22.5 mol% C_6D_6 , 22.5 mol% C_6H_6 , 27.5 mol% CD_3OD , 27.5 mol% CD_3OH ($1.75 \times 10^{-6} \text{ \AA}^{-2}$)
- (7) 22.5 mol% C_6D_6 , 22.5 mol% C_6H_6 , 55.0 mol% CD_3OD ($2.51 \times 10^{-6} \text{ \AA}^{-2}$)
- (8) 45 mol% C_6H_6 , 55 mol% CD_3OH ($3.10 \times 10^{-6} \text{ \AA}^{-2}$)
- (9) 45 mol% C_6H_6 , 55 mol% CD_3OD ($4.63 \times 10^{-6} \text{ \AA}^{-2}$)
- (10) 45 mol% C_6D_6 , 55 mol% CH_3OH ($5.81 \times 10^{-6} \text{ \AA}^{-2}$)

2 Neutron scattering experiments

$\text{Ti}_{0.68}\text{Zr}_{0.32}$ null-scattering alloy sample cells with internal dimensions of $1 \times 38 \times 38$ mm were used to contain the azeotropic mixtures during the neutron scattering measurements. These were carried out at 25°C for $\sim 1000 \mu\text{A h}$ of proton current on the SANDALS and NIMROD instruments at the ISIS spallation neutron source at the Rutherford Appleton Laboratory, UK.⁴ SANDALS detects neutrons scattered at angles between 3.9 and 39° , and covers a wavevector-transfer range of 0.1 – 50 \AA^{-1} . NIMROD detects neutrons scattered at angles between 0.5 and 40° , and covers a wavevector-transfer range of 0.02 – 50 \AA^{-1} . The

wavevector transfer, Q , is calculated from the wavelengths of the incident neutrons, λ , and their scattering angles, 2θ , according to:

$$Q = \frac{4\pi}{\lambda} \sin \theta \quad \text{Eq. S1}$$

To make the scattering data suitable for structural modelling the raw data were first corrected for absorption and multiple scattering using the *GudrunN* software package which was also used to subtract the perturbation to the data caused by inelastic scattering.⁵ These inelasticity features were removed using the *Iterate Gudrun* routine in *GudrunN* to give the total structure factors, $F(Q)$ s, of the liquids.

3 Empirical Potential Structural Refinement

To produce suitable starting structures for modelling the experimental diffraction data a standard Monte Carlo simulation was first carried out using the EPSR (Empirical Potential Structure Refinement) program.^{6,7} For the acetone-chloroform azeotrope, a cubic box with an edge length of 125.143 Å was filled with 9020 chloroform and 6140 acetone molecules giving an atomic density of 0.054341 Å⁻³.² For the benzene-methanol azeotrope the simulation box had an edge length of 123.223 Å, and contained 8100 benzene and 9900 methanol molecules giving an atomic density of 0.083698 Å⁻³. The labelling of the various atom types of acetone, benzene, chloroform and methanol molecules is shown in Figure S1.

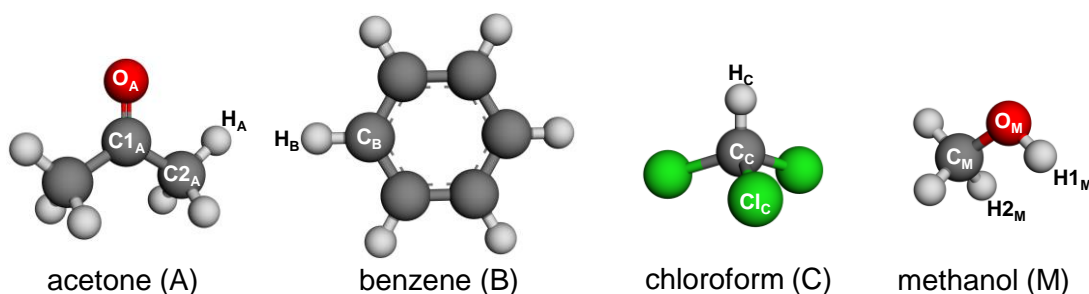


Figure S1 Molecular structures of acetone, benzene, chloroform and methanol including the labelling of the various atom types used for this study.

The average bond lengths and angles of acetone were taken from the EPSR study of the pure liquid.⁸ The average bond lengths and angles of methanol as well as benzene along with 12-6 Lennard-Jones parameters and partial charges for acetone, methanol and benzene were taken from the literature on *Transferable Potentials for Phase Equilibria (TraPPE)*⁹⁻¹¹ (cf. Table S1-S3).

Table S1 Structural parameters of acetone molecules used for the starting configuration of the EPSR simulation. Average bond lengths, r_{A-B} , and angles, γ_{A-B-C} , Lennard-Jones parameters, σ and ε , and partial charges, q .^{8,9}

$r_{C1A-C1A} / \text{Å}$	1.500			
$r_{C2A-HA} / \text{Å}$	1.085			
$r_{C1A-OA} / \text{Å}$	1.210			
$\gamma_{C2A-C1A-C2A} / ^\circ$	118.00			
$\gamma_{C2A-C1A-OA} / ^\circ$	121.00			
$\gamma_{HA-C2A-HA} / ^\circ$	110.00			
$\sigma / \text{Å}$	C1 _A : 3.75	C2 _A : 3.82	O _A : 3.05	H _A : 0.00
$\varepsilon / \text{kJ mol}^{-1}$	C1 _A : 0.33256	C2 _A : 0.81482	O _A : 0.65684	H _A : 0.00
q / e	C1 _A : 0.424	C2 _A : 0.00	O _A : -0.424	H _A : 0.00

Table S2 Structural parameters of methanol molecules used for the starting configuration of the *EPSR* simulation. Average bond lengths, r_{A-B} , and angles, γ_{A-B-C} , Lennard-Jones parameters, σ and ε , and partial charges, q .¹⁰

$r_{CM-OM} / \text{\AA}$	1.430			
$r_{CM-HM} / \text{\AA}$	1.0936			
$r_{OM-H1M} / \text{\AA}$	0.945			
$\gamma_{CM-OM-H1M} / ^\circ$	108.50			
$\gamma_{H2M-CM-H2M} / ^\circ$	108.63			
$\gamma_{H2M-CM-OM} / ^\circ$	110.30			
$\sigma / \text{\AA}$	$C_M: 3.75$	$H1_M: 0$	$H2_M: 0$	$O_M: 3.02$
$\varepsilon / \text{kJ mol}^{-1}$	$C_M: 0.81482$	$H1_M: 0$	$H2_M: 0$	$O_M: 0.77324$
q / e	$C_M: 0.265$	$H1_M: 0.435$	$H2_M: 0$	$O_M: -0.700$

Table S3 Structural parameters of benzene molecules used for the starting configuration of the *EPSR* simulation. Average bond lengths, r_{A-B} , angles, γ_{A-B-C} , and dihedral angles, $\gamma_{A-B-C-D}$, Lennard-Jones parameters, σ and ε , and partial charges, q .¹¹

$r_{CB-CB} / \text{\AA}$	1.400		
$r_{CB-HB} / \text{\AA}$	1.080		
$\gamma_{CB-CB-CB} / ^\circ$	120.00		
$\gamma_{CB-CB-HB} / ^\circ$	120.00		
$\gamma_{CB-CB-CB-CB} / ^\circ$	0.00		
$\gamma_{CB-CB-CB-HB} / ^\circ$	180.00		
$\gamma_{HB-CB-CB-HB} / ^\circ$	0.00		
$\sigma / \text{\AA}$	$C_B: 3.695$	$H_B: 0.0$	
$\varepsilon / \text{kJ mol}^{-1}$	$C_B: 0.41988$	$H_B: 0.0$	
q / e	$C_B: 0.0$	$H_B: 0.0$	

The average bond lengths and angles of chloroform were taken from microwave experiments.¹² The 12-6 Lennard-Jones parameters and partials charges for chloroform were determined by Chang *et. al.*¹³ (*cf.* Table S4).

Table S4 Structural parameters of chloroform molecules used for the starting configuration of the *EPSR* simulation. Average bond lengths, r_{A-B} , and angles, γ_{A-B-C} , Lennard-Jones parameters, σ and ε , and partial charges, q .^{12, 13}

$r_{CC-ClC} / \text{\AA}$	1.765		
$r_{CC-HC} / \text{\AA}$	1.085		
$\gamma_{ClC-CC-ClC} / ^\circ$	111.00		
$\gamma_{ClC-CC-HC} / ^\circ$	107.90		
$\sigma / \text{\AA}$	$C_C: 3.41$	$H_C: 2.81$	$Cl_C: 3.45$
$\varepsilon / \text{kJ mol}^{-1}$	$C_C: 0.5732$	$H_C: 0.08364$	$Cl_C: 1.1522$
q / e	$C_C: 0.5609$	$H_C: -0.0551$	$Cl_C: -0.16286$

The structural models of the acetone-chloroform and benzene-methanol azeotropes contain 8 and 6 distinct atom types, respectively. Consequently, for the acetone-chloroform azeotrope 28 pair-correlation

functions, $g_{ij}(r)$, are obtained from the model and for the benzene-methanol azeotrope there are 21. These are related to the corresponding partial structure factors, $S_{ij}(Q)$, by Fourier sine transform¹⁴

$$S_{ij}(Q) = 1 + \frac{4\pi\rho_0}{Q} \int_0^\infty r [g_{ij}(r) - 1] \sin(Qr) dr \quad \text{Eq. S2}$$

where ρ_0 is the atomic number density. The total structure factor, $F(Q)$, can then be calculated from the weighted sums of the partial structure factors.

$$F(Q) = \sum_{i \leq j} (2 - \delta_{ij}) w_{ij} (S_{ij}(Q) - 1) \quad \text{Eq. S3}$$

The Kronecker delta, δ_{ij} , ensures that ‘like’ terms, for which $A = B$, are not counted twice. The weighting factors, w_{ij} , by which the partial structure factors contribute to $F(Q)$ depend on the atomic fractions of the different types of atoms, c_i , and their neutron scattering lengths b_i .¹⁴

$$w_{ij} = c_i c_j b_i b_j \quad \text{Eq. S4}$$

The weighting factors of the various atom pairs for the different liquid mixtures are given in Tables S5-6. Due to the difference in neutron scattering length between ¹H (−3.74 fm) and D (6.67 fm) all $S_{ij}(Q)$ s related to H contribute differently to the $F(Q)$ s of the isotopically different liquids. In principle, to fully describe the structure of the liquid mixtures all $S_{ij}(Q)$ s need to be known. However, since only a limited number of $F(Q)$ s with different hydrogen contrasts are available from our experiment, EPSR is required to estimate some of the missing structural information. To prepare the final structural model EPSR compares simulated $F(Q)$ data with the experimental $F(Q)$ s and introduces so-called empirical potentials between the atom pairs in the structural model in an iterative process until the simulated $F(Q)$ s provide the best possible fit to the experimental $F(Q)$ s. At least 1000 model iterations were then used to accumulate the $g_{ij}(r)$ and other structural data from the EPSR models.

Table S5 Weighting factors in $\text{b sr}^{-1} \text{atom}^{-1}$ and weighting factors normalised by $\langle b \rangle^2 \times 10^{-2}$ indicating the contributions of each atom pair to the measured diffraction data of the acetone-chloroform liquid mixtures. The coherent $\langle b \rangle^2$ and total $\langle b^2 \rangle$ cross sections ($\text{b sr}^{-1} \text{atom}^{-1}$) are also indicated.

	CD_3COCD_3 CDCl_3		CH_3COH_3 CDCl_3		CH_3COCH_3 CHCl_3		CD_3COCD_3 CHCl_3		$\text{C(H/D)}_3\text{COC(H/D)}_3$ CDCl_3		CD_3COCD_3 C(H/D)Cl_3		$\text{C(H/D)}_3\text{COC(H/D)}_3$ C(H/D)Cl_3	
$\text{C1}_A\text{-C1}_A$	0.0015	0 %	0.0015	1	0.0015	2	0.0015	0	0.0015	0	0.0015	0	0.0015	1
$\text{C1}_A\text{-C2}_A$	0.0059	1 %	0.0059	4	0.0059	7	0.0059	1	0.0059	2	0.0059	1	0.0059	2
$\text{C1}_A\text{-H}_A$	0.0177	3 %	-0.0099	-7	-0.0099	-12	0.0177	4	0.0039	1	0.0177	4	0.0039	1
$\text{C1}_A\text{-O}_A$	0.0026	0 %	0.0026	2	0.0026	3	0.0026	1	0.0026	1	0.0026	1	0.0026	1
$\text{C2}_A\text{-C2}_A$	0.0059	1 %	0.0059	4	0.0059	7	0.0059	1	0.0059	2	0.0059	1	0.0059	2
$\text{C2}_A\text{-H}_A$	0.0353	7 %	-0.0198	-14	-0.0199	-24	0.0354	8	0.0077	3	0.0353	7	0.0077	3
$\text{C2}_A\text{-O}_A$	0.0051	1 %	0.0051	4	0.0051	6	0.0051	1	0.0051	2	0.0051	1	0.0051	2
$\text{H}_A\text{-H}_A$	0.0532	10 %	0.0167	12	0.0168	20	0.0533	13	0.0026	1	0.0532	11	0.0025	1
$\text{H}_A\text{-O}_A$	0.0154	3 %	-0.0086	-6	-0.0087	-11	0.0155	4	0.0034	1	0.0154	3	0.0034	1
$\text{O}_A\text{-O}_A$	0.0011	0 %	0.0011	1	0.0011	1	0.0011	0	0.0011	0	0.0011	0	0.0011	0
$\text{C}_C\text{-C}_C$	0.0032	1 %	0.0032	2	0.0032	4	0.0032	1	0.0032	1	0.0032	1	0.0032	1
$\text{C}_C\text{-H}_C$	0.0064	1 %	0.0064	5	-0.0036	-4	-0.0036	-1	0.0064	2	0.0014	0	0.0014	1
$\text{C}_C\text{-Cl}_C$	0.0274	5 %	0.0274	19	0.0273	33	0.0273	7	0.0274	9	0.0274	6	0.0274	11
$\text{H}_C\text{-H}_C$	0.0032	1 %	0.0032	2	0.0010	1	0.0010	0	0.0032	1	0.0002	0	0.0002	0
$\text{H}_C\text{-Cl}_C$	0.0275	5 %	0.0275	20	-0.0154	-19	-0.0154	-4	0.0275	9	0.0060	1	0.0060	2
$\text{Cl}_C\text{-Cl}_C$	0.0590	11 %	0.0590	42	0.0589	72	0.0588	14	0.0591	19	0.0591	12	0.0592	23
$\text{C1}_A\text{-C}_C$	0.0043	1 %	0.0043	3	0.0043	5	0.0043	1	0.0043	1	0.0043	1	0.0043	2
$\text{C1}_A\text{-H}_C$	0.0043	1 %	0.0043	3	-0.0024	-3	-0.0024	-1	0.0043	1	0.0010	0	0.0010	0
$\text{C1}_A\text{-Cl}_C$	0.0186	3 %	0.0186	13	0.0186	23	0.0186	4	0.0186	6	0.0186	4	0.0186	7
$\text{C2}_A\text{-C}_C$	0.0086	2 %	0.0086	6	0.0086	11	0.0086	2	0.0086	3	0.0086	2	0.0086	3
$\text{C2}_A\text{-H}_C$	0.0087	2 %	0.0087	6	-0.0049	-6	-0.0049	-1	0.0087	3	0.0019	0	0.0019	1
$\text{C2}_A\text{-Cl}_C$	0.0372	7 %	0.0372	26	0.0372	45	0.0372	9	0.0372	12	0.0372	8	0.0372	14
$\text{H}_A\text{-C}_C$	0.0260	5 %	-0.0146	-10	-0.0146	-18	0.0260	6	0.0057	2	0.0260	5	0.0057	2
$\text{H}_A\text{-H}_C$	0.0261	5 %	-0.0146	-10	0.0082	10	-0.0146	-3	0.0057	2	0.0057	1	0.0013	0
$\text{H}_A\text{-Cl}_C$	0.1121	21 %	-0.0629	-45	-0.0628	-77	0.1120	27	0.0245	8	0.1121	23	0.0246	9
$\text{O}_A\text{-C}_C$	0.0038	1 %	0.0038	3	0.0038	5	0.0038	1	0.0038	1	0.0038	1	0.0038	1
$\text{O}_A\text{-H}_C$	0.0038	1 %	0.0038	3	-0.0021	-3	-0.0021	-1	0.0038	1	0.0008	0	0.0008	0
$\text{O}_A\text{-Cl}_C$	0.0163	3 %	0.0163	12	0.0162	20	0.0162	4	0.0163	5	0.0163	3	0.0163	6
$\langle b \rangle^2$	0.5400		0.1405		0.0820		0.4181		0.3077		0.4771		0.2609	
$\langle b^2 \rangle$	0.7348		2.7814		3.2840		1.2352		1.7588		0.9859		2.0094	

Table S6 Weighting factors in $\text{b sr}^{-1} \text{atom}^{-1}$ and weighting factors normalised by $\langle b \rangle^2 \times 10^{-2}$ indicating the contributions of each atom pair to the measured diffraction data of the benzene-methanol liquid mixtures. The coherent $\langle b \rangle^2$ and total $\langle b^2 \rangle$ cross sections ($\text{b sr}^{-1} \text{atom}^{-1}$) are also indicated.

	C_6D_6 CD_3OD		C_6D_6 CD_3OH		C_6D_6 $\text{CD}_3\text{O(H/D)}$		C_6H_6 CD_3OD		$\text{C}_6(\text{H/D})_6$ CD_3OD		C_6H_6 CD_3OH		$\text{C}_6(\text{H/D})_6$ $\text{CD}_3\text{O(H/D)}$		C_6H_6 CH_3OH		$\text{C}_6(\text{H/D})_6$ $\text{C(H/D)}_3\text{O(H/D)}$		C_6D_6 CH_3OH	
$\text{C}_R\text{-C}_R$	0.0426	10%	0.0425	12	0.0422	11	0.0425	37	0.0424	17	0.0426	57	0.0425	19	0.0422	771	0.0425	31	0.0425	27
$\text{C}_R\text{-C}_M$	0.0173	4%	0.0173	5	0.0174	4	0.0173	15	0.0173	7	0.0173	23	0.0173	8	0.0174	313	0.0173	13	0.0173	11
$\text{C}_R\text{-O}_M$	0.0151	3%	0.0151	4	0.0152	4	0.0151	13	0.0151	6	0.0151	20	0.0151	7	0.0152	274	0.0151	11	0.0151	10
$\text{C}_R\text{-H}_R$	0.0855	20%	0.0852	24	0.0848	22	-0.0478	-42	0.0188	8	0.0855	-64	0.0852	9	0.0848	-867	-0.0478	14	0.0854	54
$\text{C}_R\text{-H}2_M$	0.0522	12%	0.0522	15	0.0523	13	0.0522	46	0.0522	21	0.0522	71	0.0522	24	0.0523	-529	0.0522	9	-0.0293	-19
$\text{C}_R\text{-H}2_M$	0.0174	4%	-0.0098	-3	0.0038	1	0.0174	15	0.0174	7	0.0174	-13	-0.0098	2	0.0038	-176	0.0174	3	-0.0098	-6
$\text{C}_M\text{-C}_M$	0.0018	0%	0.0018	1	0.0018	0	0.0018	2	0.0018	1	0.0018	2	0.0018	1	0.0018	32	0.0018	1	0.0018	1
$\text{C}_M\text{-O}_M$	0.0031	1%	0.0031	1	0.0031	1	0.0031	3	0.0031	1	0.0031	4	0.0031	1	0.0031	56	0.0031	2	0.0031	2
$\text{C}_M\text{-H}_R$	0.0174	4%	0.0174	5	0.0174	4	-0.0098	-9	0.0038	2	0.0174	-13	0.0174	2	0.0174	-176	-0.0098	3	0.0174	11
$\text{C}_M\text{-H}2_M$	0.0106	2%	0.0107	3	0.0108	3	0.0107	9	0.0107	4	0.0106	14	0.0107	5	0.0108	-108	0.0107	2	-0.0060	-4
$\text{C}_M\text{-H}1_M$	0.0035	1%	-0.0020	-1	0.0008	0	0.0036	3	0.0036	1	0.0035	-3	-0.0020	0	0.0008	-36	0.0036	1	-0.0020	-1
$\text{O}_M\text{-O}_M$	0.0013	0%	0.0014	0	0.0014	0	0.0013	1	0.0014	1	0.0013	2	0.0014	1	0.0014	24	0.0013	1	0.0013	1
$\text{O}_M\text{-H}_R$	0.0152	3%	0.0152	4	0.0152	4	-0.0085	-7	0.0034	1	0.0152	-12	0.0152	2	0.0152	-154	-0.0085	2	0.0152	10
$\text{O}_M\text{-H}2_M$	0.0093	2%	0.0093	3	0.0094	2	0.0093	8	0.0093	4	0.0093	13	0.0093	4	0.0094	-94	0.0093	2	-0.0052	-3
$\text{O}_M\text{-H}1_M$	0.0031	1%	-0.0017	0	0.0007	0	0.0031	3	0.0031	1	0.0031	-2	-0.0017	0	0.0007	-31	0.0031	1	-0.0017	-1
$\text{H}_R\text{-H}_R$	0.0429	10%	0.0428	12	0.0426	11	0.0135	12	0.0021	1	0.0429	18	0.0428	1	0.0426	244	0.0135	2	0.0429	27
$\text{H}_R\text{-H}_M$	0.0524	12%	0.0524	15	0.0525	13	-0.0294	-26	0.0116	5	0.0524	-40	0.0524	5	0.0525	298	-0.0294	2	-0.0294	-19
$\text{H}_R\text{-H}1_M$	0.0175	4%	-0.0098	-3	0.0039	1	-0.0098	-9	0.0039	2	0.0175	7	-0.0098	0	0.0039	99	-0.0098	1	-0.0098	-6
$\text{H}2_M\text{-H}2_M$	0.0160	4%	0.0161	5	0.0162	4	0.0161	14	0.0161	6	0.0160	22	0.0161	7	0.0162	91	0.0161	1	0.0050	3
$\text{H}2_M\text{-H}1_M$	0.0107	2%	-0.0060	-2	0.0024	1	0.0107	9	0.0107	4	0.0107	-8	-0.0060	1	0.0024	61	0.0107	0	0.0034	2
$\text{H}1_M\text{-H}1_M$	0.0018	0%	0.0006	0	0.0001	0	0.0018	2	0.0018	1	0.0018	1	0.0006	0	0.0001	10	0.0018	0	0.0006	0
$\langle b \rangle^2$	0.4365		0.3537		0.3939		0.1141		0.2496		0.0741		0.2177		0.0055		0.1350		0.1579	
$\langle b^2 \rangle$	0.5287		0.9035		0.7168		2.3640		1.4444		2.7366		1.6319		3.8621		2.1955		2.0255	

4 Classification of local environments in the EPSR models

The state of mixing of the two components A and B in binary azeotropic mixtures has profound consequence on the physicochemical properties. In order to describe the local molecular environments in binary mixtures in an accessible fashion we classify them as AA , AB , BA or BB . This is carried out by our LENCA (Local ENvironment ClAssification) computer program which analyses a given simulation box containing the centre-of-mass coordinates of the A and B molecules of a binary mixture. The first letter in this classification scheme indicates the type of molecule under consideration and the second letter designates the species that dominates the local environment. The condition for dominating a local environment is that the first coordination shell contains more of the species in question than the other component. In the unlikely case that the same numbers of A and B molecules are found in a given local environment LENCA makes a random decision.

To illustrate this kind of analysis we first investigate ideal gas mixtures which have randomly placed molecules. For these mixtures, there is no defined first coordination shell and therefore an arbitrary distance was chosen to define the local environment. In fact, the distance over which the local environments are analysed does not influence the outcome of our analysis as long as this distance is the same for both species and all environments. Figure S2 shows how the local environments change as the mole fraction of A molecules, x_A , increases.

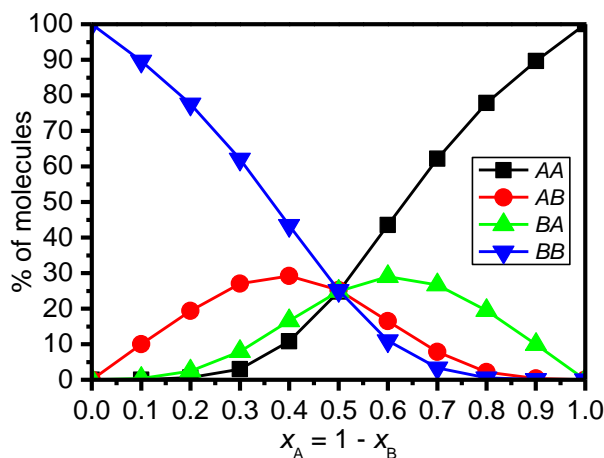


Figure S2 Percentages of molecules found in AA , AB , BA and BB local environments as a function of the composition of a binary mixture of ideal gases.

As expected, only BB environments are found at $x_A = 0$. Upon increasing x_A to 0.1 the percentage of BB environments decreases by about 10% since the mole fraction of B decreases. Owing to the small amounts of A at $x_A = 0.1$ very few BA environments exist. The local environments of A are initially almost all AB . The chances of finding AA environments are very small. Upon increasing x_A to 0.5 the percentage of BB environments decreases substantially, and increasing numbers of AB , BA and AA environments are found. At $x_A = 0.5$ equal percentages of all four environments, *i.e.* 25%, are found as expected. Upon further increasing x_A , the AA environments begin to dominate and the percentages of all other local environments tend to zero as x_A approaches one. In Figure S3, the changes in environments are shown from the perspective of A molecules only.

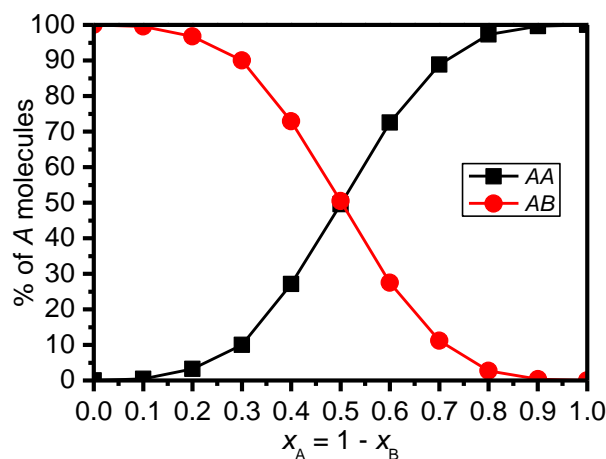


Figure S3 Percentages of A molecules in AA and AB environments as a function of x_A .

Figure 7 in the main article shows the results from such an analysis of local environments for the *EPSR* models of the acetone-chloroform and benzene-methanol azeotropes. In order to account for the different molecular volumes of the various chemical species in the azeotropes the distance ranges of the first coordination shells, *i.e.* $0 \rightarrow r_1$, were individually determined from the minima after the first peak in the $g_{\text{COM-COM}}(r)$ functions shown in Figure 8. Specifically, the r_1 values chosen for the acetone-chloroform azeotrope were $r_1(\text{AA}) = 6.949 \text{ \AA}$, $r_1(\text{AC}) = 7.317 \text{ \AA}$, $r_1(\text{CC}) = 7.360 \text{ \AA}$, and for the benzene-methanol azeotrope $r_1(\text{BB}) = 7.747 \text{ \AA}$, $r_1(\text{BM}) = 6.540 \text{ \AA}$, $r_1(\text{MM}) = 5.692 \text{ \AA}$. Choosing larger distances for pair-correlations involving species with larger molecular volumes is important so that these species have an equal chance to be the ‘winner’ when it comes to assigning the local environment. As shown in Figures S2 and S3, our analysis of local molecular environments depends strongly on the composition of the mixture. It is therefore important to compare the determined percentages of the local environments of the azeotropes with the grey bars in Figure 7 which denote the expected fractions of local environments for the corresponding random mixtures at the same mole fractions as the azeotropes.

5 X-ray diffraction and differential scanning calorimetry upon cooling

Acetone-chloroform and benzene-methanol azeotropes show different behaviour upon cooling. The changes in heat flow and phase transitions of the azeotropes during cooling from 290 K to 80 K are shown in the DSC scans and variable temperature X-ray diffraction contour plots of Figure S4. For the acetone-chloroform azeotrope there is a subtle increase in diffracted intensity between 15-30 degrees upon cooling and the DSC scan is featureless apart from an endothermic step at $\sim 120 \text{ K}$. Whilst the increase in diffracted intensity indicate some structural changes in liquid structure, the absence of Bragg peaks in the diffraction data and endothermic peaks in the DSC scan indicate that this system does not crystallise upon cooling. The endothermic step was found to be reversible upon subsequent heating indicating that this system forms a glass with a glass transition temperature, T_g , of 118.9 K ($\Delta C_p = 0.54 \text{ J g}^{-1}$). It can be speculated that the glass transition of the benzene-methanol azeotrope prevents the phase separation into two liquids at low temperatures. Such behaviour is frequently observed for positive azeotropes due to the unfavourable interactions between unlike species.¹⁵

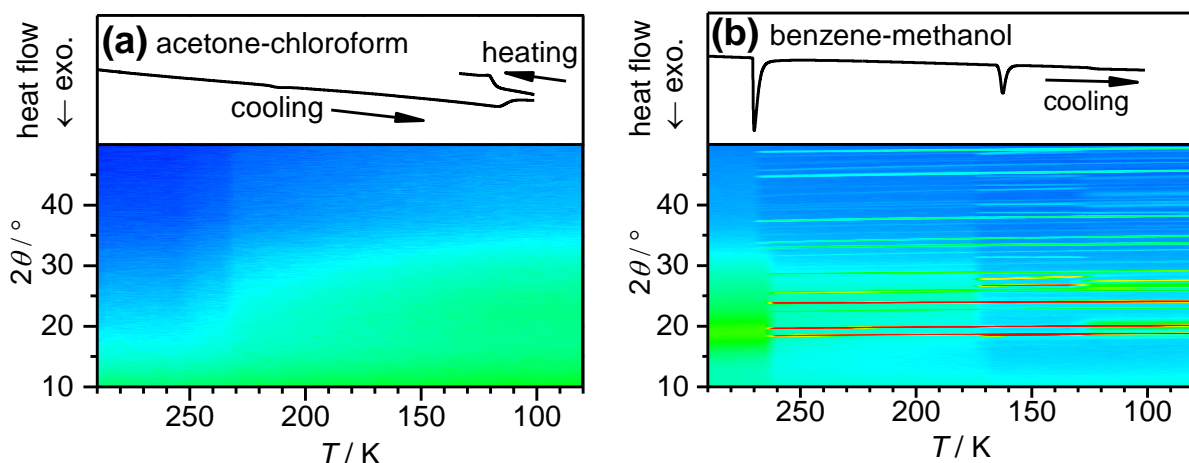


Figure S4 Differential scanning calorimetry scans (10 K min^{-1}) and contour plots showing X-Ray diffractograms (15 K h^{-1}) recorded upon cooling (a) the acetone-chloroform and (b) benzene methanol azeotropes. A DSC scan recorded upon subsequent heating of the acetone-chloroform glass more clearly shows its glass transition temperature at 118.9 K .

The binary phase diagram of acetone and chloroform has also been explored by other researchers.^{16, 17 18} Upon cooling the benzene-methanol azeotrope there are two pronounced exothermic peaks in the DSC scan with onsets at 270.6 K ($7658.9 \text{ kJ mol}^{-1}$) and 164.2 K ($2502.2 \text{ kJ mol}^{-1}$), respectively, followed by a subtle step in heat flow at 126.2 K . The position of the emerging Bragg peaks indicate that these are due to the sequential crystallisation of benzene¹⁹ and then methanol,²⁰ which later undergoes a solid-solid phase transition to its low temperature form.²¹

6 Calculation of Kirkwood-Buff integrals from thermodynamic data

The double-iterative Barker method was used to calculate chemical potentials from measurements of total vapour pressure.²² The variation in the activity coefficients, γ_1 and γ_2 with composition x_1 and x_2 were fitted with second order polynomials.

$$\ln \gamma_1 = A x_2^2 - B x_2^2(1 - 4x_1) + C x_2^2(1 - 8x_1 + 12x_1^2)$$

$$\ln \gamma_2 = A x_1^2 + B x_1^2(1 - 4x_2) + C x_1^2(1 - 8x_2 + 12x_2^2)$$

Eq. S5-6

To find the best-fit values for the A , B and C constants, the residuals of the measured total vapour pressure, p_{meas} , and that calculated, p_{calc} , from Eq. S7 were minimised using a least-squares approach. The vapour pressures of the pure liquids are p_1 and p_2 , V_1 and V_2 are the molar volumes of the pure liquids, B_{11} and B_{22} are the second virial coefficients of the pure liquids, and B_{12} is the cross virial term for the mixtures. The values used are given in Table S7. R is the gas constant and T the temperature. The total pressure, p , as well as y_1 and y_2 , the mole fractions of the vapour phase, were updated iteratively until convergence was achieved. Measured values were used in the first instance, later being replaced with those calculated from the least squares fit. Changing the value of B_{12} from a value midway between B_{11} and B_{22} had only a small

effect on the result. The pressure isotherm data used are given in Tables S8-9. The agreement of calculated and measured pressure is shown in Figure S5.

$$p_{calc} = x_1\gamma_1 \exp[\{(V_1 - B_{11})(p - p_1) - p y_2^2(2B_{12} - B_{11} - B_{22})\}/RT] \\ + x_2\gamma_2 \exp[\{(V_2 - B_{22})(p - p_2) - p y_1^2(2B_{12} - B_{11} - B_{22})\}/RT]$$

Eq. S7

The formulae of Żółkiewski²³ (Eqs S8-12) were used to calculate G_{11} , G_{12} and G_{22} , the Kirkwood-Buff integrals of binary mixtures. Their variations with composition are shown in Figure S6. The values at the azeotropic composition are given in Table S7. v_1 and v_2 are partial molar volumes, ρ_1 and ρ_2 are the molar densities of the components in the mixture, where $\rho = \rho_1 + \rho_2$ is the total density, β_T is the isothermal compressibility of the mixture, and μ_1 and μ_2 are the chemical potentials ($\mu_1 = \ln x_1\gamma_1$ and $\mu_2 = \ln x_2\gamma_2$).

$$\eta = RT \left(\frac{\rho^2}{\rho_2}\right) / \left(\frac{d\mu_2}{dx_2}\right) = RT \left(\frac{\rho^2}{\rho_1}\right) / \left(\frac{d\mu_1}{dx_1}\right) \text{ and } \xi = RT\beta_T\eta$$

$$G_{12} = (\xi - \eta v_1 v_2) / \eta$$

$$G_{11} = G_{12} + (\eta v_2 - 1) / \rho_1$$

$$G_{22} = G_{12} + (\eta v_1 - 1) / \rho_2$$

Eq. S8-12

The derivatives of the chemical potential of 2nd components with respect to composition were constructed directly from the functional form of the activity coefficients described by Eq. S5-6.

$$\frac{d\mu_2}{dx_2} = [48C x_2^4 + (-96C - 12B)x_2^3 + (58C + 18B + 2A)x_2^2 + (-10C - 6B - 2A)x_2 + 1] / x_2$$

Eq. S13

The densities of the components were calculated from the total density found using the excess volumes, V^E , and the densities of the pure components (Table S7). Eq. S14 was used to express the variation of excess volume with composition. The excess volume data used for the fit are given in Tables S10-11. The values of a and b are given in Table S7. The quality of fit is shown in Figure S5. Good quality data was not available for the benzene-methanol system at 308.15 K, 318.15 K or 328.15 K. For these temperatures, data collected at 313.15 K was used. The partial molar volumes are the derivative of volume with respect to the amount of component 2, n_2 , in a mixture where $n_1 = 1$ and $n_2 = x_1/x_2$.

$$V^E = x_1 x_2 [a - b(1 - 2x_2)]$$

Eq. S14

The isothermal compressibility of the mixtures, β_T , was estimated from the excess molar volume and the isothermal compressibility of the pure components, β_1 and β_2 (Table S7), using Eq. S15-17. As the influence of pressure on the excess volume was not available the last term in Eq. S15 was assumed to be zero.

$$\beta_T = \phi_1\beta_1 + \phi_2\beta_2 - V_m^{-1}(dV^E/dp)_T$$

$$\phi_i = x_iV_i/V_m$$

$$V_m = x_1V_1 + x_2V_2 + V^E$$

Eq. S15-17

The error introduced into the Kirkwood-Buff integral with this simplification and the approximation of excess mixing volume of benzene-methanol mixtures at higher temperatures is expected to be no greater than 1-2 Å³ molecule⁻¹. The greatest contribution to the overall error is from the derivative of the chemical potential and thus from the quality of the vapour-pressure composition data. In order to ensure a physically meaningful positive value of the derivative of chemical potential over the entire concentration range for the benzene-methanol system at 298.15 K, it was necessary to exclude measurements of the most concentrated benzene mixtures from the fit. This approach was chosen over placing limits on the allowable values of the derivative of chemical potential as it has been suggested that these data points may have significant experimental uncertainty due to the difficulty of reaching an equilibrium.²⁴

Table S7 Values used for the calculation of Kirkwood-Buff integrals. The vapour pressure, p , and density ρ of the pure components were taken from the Dortmund data bank online resource. Where available, the pure component vapour pressure measurements of the original authors were used (see Tables S8-9). The second virial coefficients of the pure liquids, B_{11} , were taken from Dymond and Smith.²⁵ Second virial coefficients of the mixtures, β_{12} , for acetone-chloroform were from Kearns *et al.*²⁶ and values for benzene-methanol mixtures were interpolated from the measurements of Knoebel.²⁷ β_T values were interpolated from data provided in the CRC handbook of Chemistry and Physics.²⁸

	T / K	p / kPa	$\rho / \text{g cm}^{-3}$	$B_{11} / \text{cm}^3 \text{mol}^{-1}$	$\beta_T / \text{TPa}^{-1}$
acetone	298.15	30.593	0.7858	-2051.0	1337
acetone	308.15	46.266	0.7746	-1780.5	1486
chloroform	298.15	26.221	1.4792	-1193.0	1045
chloroform	308.15	39.542	1.4608	-1100.0	1143
benzene	298.15	12.684	0.8737	-1477.0	966
benzene	308.15	19.774	0.8634	-1355.9	1047
benzene	318.15	29.809	0.8530	-1249.1	1128
benzene	328.15	43.611	0.8425	-1154.6	1209
methanol	298.15	16.915	0.7877	-1752.0	1256
methanol	308.15	27.918	0.7783	-1600.0	1341
methanol	318.15	44.483	0.7687	-1456.9	1425
methanol	328.15	68.673	0.7587	-1321.6	1510

mixture	T / K	a	b	$\beta_{12} / \text{cm}^3 \text{mol}^{-1}$
acetone-chloroform	298.15	-0.53966	-0.80458	-2702
acetone-chloroform	308.15	-0.50828	-0.69034	-2219
benzene-methanol	298.15	-0.02703	0.22060	-573.5
benzene-methanol	308.15	0.08855	0.35176	-554.5
benzene-methanol	318.15	0.08855	0.35176	-535.5
benzene-methanol	328.15	0.08855	0.35176	-516.5

mixture	T / K	A	B	C
acetone-chloroform	298.15	-0.95460	-0.23274	-0.04454
acetone-chloroform	308.15	-0.89270	-0.14224	-0.03913
benzene-methanol	298.15	2.00695	0.24276	0.28076
benzene-methanol	308.15	1.97284	0.23343	0.26816
benzene-methanol	318.15	1.92746	0.23687	0.26053
benzene-methanol	328.15	1.89302	0.21800	0.29067

azeotrope	T / K	$G_{11} / \text{\AA}^3 \text{molecule}^{-1}$	$G_{22} / \text{\AA}^3 \text{molecule}^{-1}$	$G_{12} / \text{\AA}^3 \text{molecule}^{-1}$
$x_A = 0.405$	298.15	-180	-160	-79
$x_A = 0.405$	308.15	-178	-160	-82
$x_M = 0.550$	298.15	83	817	-552
$x_M = 0.550$	308.15	67	775	-529
$x_M = 0.550$	318.15	40	691	-497
$x_M = 0.550$	328.15	7	591	-428

Table S8 Variation in pressure with liquid and vapour compositions in acetone-chloroform binary mixtures.

298.15 K			298.15 K			308.15 K		
<i>Zawidski</i> ¹			<i>Campbell et. al.</i> ¹⁸			<i>Apelblat et. al.</i> ²		
x_A	y_A	p / kPa	x_A	y_A	p / kPa	x_A	y_A	p / kPa
0	0	26.46	0.0000	0.000	26.291	0	0	39.93
0.094	0.064	24.6	0.1138	0.068	24.331	0.128	0.079	37.22
0.216	0.162	22.82	0.2714	0.227	22.331	0.160	0.105	35.97
0.293	0.245	22.12	0.3499	0.332	21.665	0.250	0.187	34.88
0.353	0.327	21.64	0.4750	0.520	21.998	0.378	0.378	34.09
0.405	0.405	21.52	0.6000	0.689	23.331	0.456	0.501	34.30
0.48	0.545	22.48	0.6834	0.787	24.665	0.578	0.671	35.93
0.593	0.682	23.74	0.8239	0.890	27.438	0.706	0.807	38.77
0.666	0.758	25.06	0.9105	0.950	28.998	0.749	0.850	39.64
0.707	0.798	25.64	1.0000	1.000	30.198	0.755	0.855	39.93
0.822	0.888	27.48				0.827	0.907	41.57
0.895	0.944	28.72				1	1	46.85
0.951	0.976	29.81						
1	1	30.73						

Table S9 Variation in pressure with liquid and vapour compositions in benzene-methanol binary mixtures.

298.15 K			318.15 K			328.15 K		
<i>Miyano et. al.</i> ³ , <i>Scratchard et al.</i> ²⁴			<i>Toghiani et al.</i> ²⁹			<i>Scratchard et al.</i> ²⁴		
x_M	y_M	p / kPa	x_M	y_M	p / kPa	x_M	y_M	p / kPa
0	0	12.71	0	0	29.894	0.0304	0.3019	62.11
0.0248	0.3275	19.00	0.0037	0.0882	32.744	0.0493	0.4051	70.28
0.0457	0.397	20.83	0.0102	0.1567	35.358	0.1031	0.4841	79.66
0.0663	0.4311	21.78	0.0161	0.2364	38.587	0.3297	0.555	88.56
0.1247	0.4747	23.10	0.0207	0.2794	40.962	0.4874	0.5845	90.08
0.2292	0.5042	23.92	0.0314	0.3391	44.231	0.4984	0.5858	90.12
0.3887	0.5272	24.34	0.0431	0.3794	46.832	0.6076	0.6078	90.45
0.4742*	0.5343*	24.36*	0.0613	0.4306	50.488	0.7898	0.6716	88.65
0.4974	0.5414	24.43	0.0854	0.4642	53.224	0.9014	0.7697	82.96
0.591	0.5563	24.43	0.1263	0.4921	55.571			
0.6868	0.578	24.35	0.1811	0.5171	57.454			
0.7676	0.6066	23.85	0.2334	0.5288	58.427			
0.8343	0.6451	23.10	0.3217	0.545	59.402			
0.8981	0.7088	21.81	0.3805	0.5538	59.802			
0.9512	0.8084	19.83	0.4201	0.559	60.015			
1	1	16.92	0.4746	0.5673	60.242			
			0.542	0.5783	60.416			
			0.5716	0.5821	60.443			
			0.6164	0.5908	60.416			
			0.6509	0.599	60.35			
			0.6793	0.6067	60.215			
			0.7259	0.6216	59.868			
			0.7575	0.6346	59.482			
			0.8171	0.6681	58.321			
			0.8744	0.7181	56.213			
			0.9033	0.7525	54.692			
			0.9264	0.7896	53.037			
			0.9497	0.8368	51.009			
			0.9594	0.8599	50.048			
			0.9707	0.8916	48.767			
			0.9804	0.9222	47.54			
			0.9895	0.9558	46.232			
			1	1	44.608			

Table S10 Excess volumes of acetone-chloroform binary mixtures.			
298.15 K		308.15 K	
<i>Anisimov³⁰ and Hubbard³¹</i>		<i>Apelblat et al.²</i>	
x_A	$V^E / \text{cm}^3 \text{mol}^{-1}$	x_A	$V^E / \text{cm}^3 \text{mol}^{-1}$
0	0	0	0
0.12	-0.100	0.0972	-0.084
0.12	-0.102	0.1609	-0.123
0.21	-0.162	0.1695	-0.128
0.21	-0.165	0.176	-0.131
0.33	-0.182	0.1943	-0.14
0.33	-0.196	0.2108	-0.146
0.43	-0.168	0.2779	-0.165
0.43	-0.172	0.3336	-0.17
0.52	-0.110	0.4139	-0.163
0.52	-0.144	0.4496	-0.156
0.61	-0.068	0.5316	-0.125
0.61	-0.100	0.7088	-0.042
0.80	0.000	0.8728	0.017
0.80	-0.002	0.905	0.02
0.91	0.006	1	0
0.91	0.018		
1	0		

Table S11 Excess volumes of benzene-methanol binary mixtures.			
298.15 K		313.15 K	
<i>Wood et. al.³²</i>		<i>Cibulka et. al.³³</i>	
x_M	$V^E / \text{cm}^3 \text{mol}^{-1}$	x_M	$V^E / \text{cm}^3 \text{mol}^{-1}$
0	0	0	0
0.12988	0.0283	0.055	0.0384
0.13461	0.0285	0.0762	0.0392
0.25397	0.0227	0.1522	0.0462
0.26234	0.0221	0.2325	0.0475
0.36777	0.0134	0.2876	0.0398
0.36893	0.0128	0.3625	0.0482
0.49280	-0.0014	0.4142	0.0337
0.49842	-0.0019	0.472	0.0232
0.61696	-0.0146	0.5205	0.0135
0.62142	-0.0145	0.615	0.0006
0.74600	-0.0200	0.6863	-0.0097
0.74890	-0.0200	0.7616	-0.0111
0.74979	-0.0197	0.8255	-0.0174
0.87456	-0.0162	0.9185	-0.0107
0.87755	-0.0156	0.9641	-0.0067
1	0	1	0

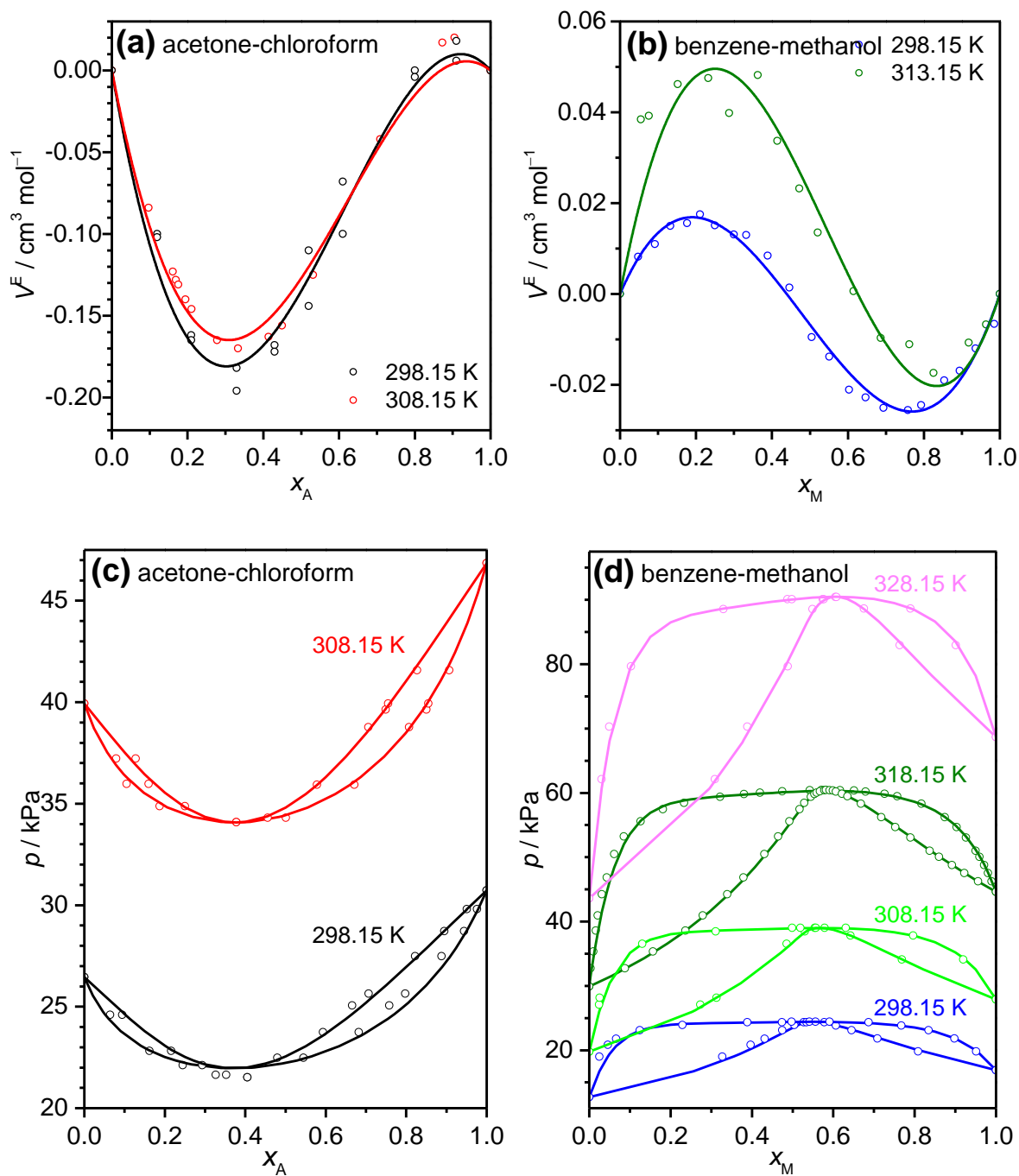


Figure S5 (a,b) Measured excess volumes and (c,d) pressure-composition phase diagrams including best-fitted functions of (a,c) acetone-chloroform and (b,d) benzene-methanol binary mixtures.

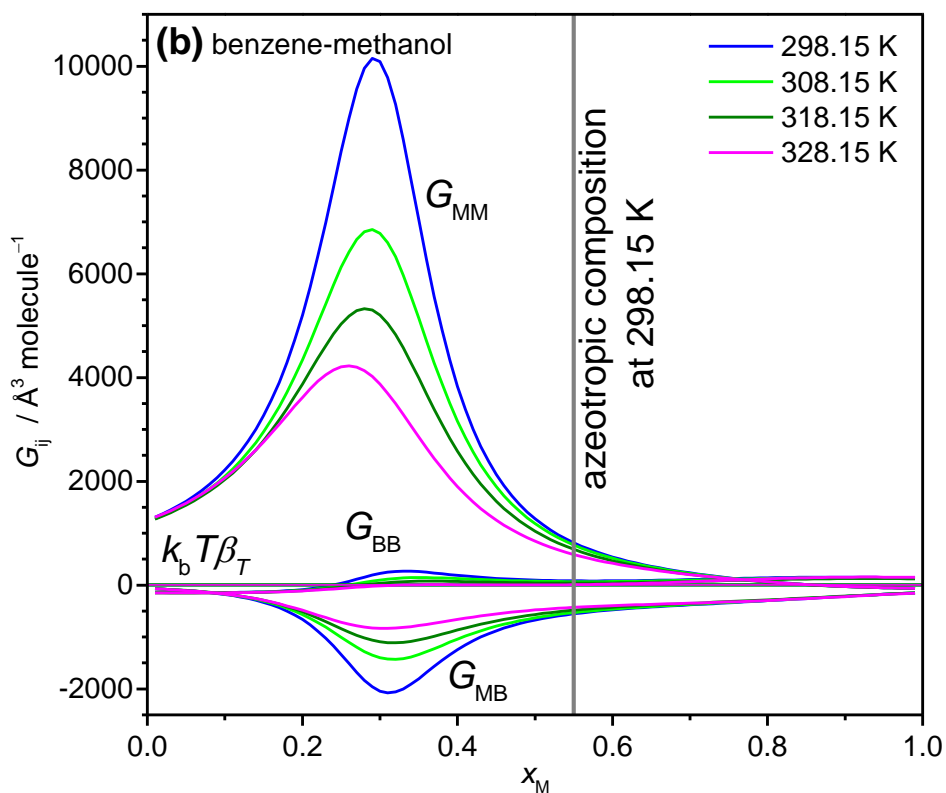
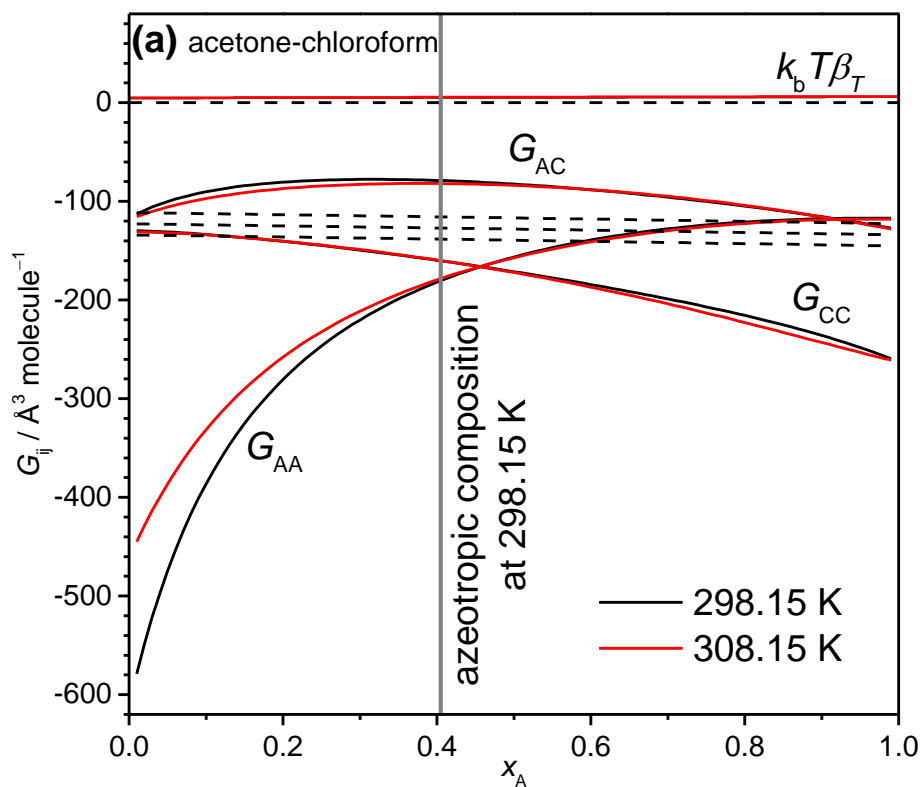


Figure S6 Kirkwood-Buff integrals for (a) acetone-chloroform binary mixtures at 298.15 K and 308.15 K, and (b) benzene-methanol binary mixtures at 298.15 K, 308.15 K, 318.15 K and 328.15 K. The variation in the Kirkwood-Buff integrals for a hypothetical ideal mixture of acetone and chloroform molecules (dashed lines) and the 298.15 K azeotropic compositions (grey line) are also indicated.

7 References

- 1 J. v. Zawidzki, *Z. Phys. Chem.*, 1900, **35**.
- 2 A. Apelblat, A. Tamir and M. Wagner, *Fluid Phase Eq.*, 1980, **4**, 229-255.
- 3 Y. Miyano and W. Hayduk, *J. Chem. Eng. Data*, 1993, **38**, 277-381.
- 4 D. T. Bowron, A. K. Soper, K. Jones, S. Ansell, S. Birch, J. Norris, L. Perrott, D. Riedel, N. J. Rhodes, S. R. Wakefield, A. Botti, M.-A. Ricci, F. Grazzi and M. Zoppi, *Rev. Sci. Instrum.*, 2010, **81**, 033905.
- 5 A. K. Soper, *Mol. Phys.*, 2009, **107**, 1667-1684.
- 6 A. K. Soper, *Chem. Phys.*, 1996, **202**, 295-306.
- 7 A. K. Soper, *Phys. Rev. B*, 2005, **72**, 104204.
- 8 S. McLain, A. K. Soper and A. Luzar, *J. Chem. Phys.*, 2006, **124**, 074502.
- 9 J. M. Stubbs, J. J. Potoff and J. I. Siepmann, *J. Phys. Chem. B*, 2004, **108**, 17596-17605.
- 10 B. Chen, J. J. Potoff and J. I. Siepmann, *J. Phys. Chem. B*, 2001, **105**, 3093-3104.
- 11 X. S. Zhao, B. Chen, S. Karaborni and a. J. I. Siepmann, *J. Phys. Chem. B*, 2005, **109**, 5368-5374.
- 12 M. Jen and D. R. Lide, *J. Chem. Phys.*, 1962, **36**, 2525-2526.
- 13 T.-M. Chang, L. X. Dang and K. A. Peterson, *J. Phys. Chem. B*, 1997, **101**, 3413-3419.
- 14 D. S. Sivia, *Elementary Scattering Theory*, Oxford University Press, Oxford, 2011.
- 15 J. S. Rowlinson and F. L. Swinton, *Liquids and Liquid Mixtures*, Butterworth Scientifics, London, Third edn., 1982.
- 16 A. N. Campbell and E. M. Kartzmark, *Can. J. Chem.*, 1960, **38**, 652-655.
- 17 G. J. Korinek and W. G. Schneider, *Can. J. Chem.*, 1957, **35**, 1157-1163.
- 18 A. N. Campbell, E. M. Kartzmark and R. M. Chatterjee, *Can. J. Chem.*, 1966, **44**, 1183-1139.
- 19 G. A. Jeffrey, J. R. Ruble, R. K. McMullan and J. A. Pople, *Proc. Natl. Acad. Sci. Lond. A*, 1987, **414**, 47-56.
- 20 K. J. Tauer and W. N. Lipscomb, *Acta Cryst.*, 1952, **5**, 606-613.
- 21 B. H. Torrie, O. S. Binbrek, M. Straussa and I. P. Swainson, *J. Solid State Chem.*, 2002, **166**, 415-420.
- 22 J. A. Barker, *Aust. J. Chem.*, 1953, **6**, 207-210.
- 23 M. Zolkiewski, *J. Solution Chem.*, 1987, **16**, 1025-1034.
- 24 G. Scratchard, S. E. Wood and J. M. Mochel, *J. Am. Chem. Soc.*, 1946, **68**.
- 25 J. H. Dymond and E. B. Smith, *The Virial Coefficients of Pure Gases and Mixtures, A Critical Compilation*, Oxford University Press, Oxford, 1980.
- 26 E. R. Kearns, *J. Phys. Chem.*, 1961, **65**, 314-316.
- 27 D. H. Knoebel and W. C. Edmister, *J. Chem. Eng. Data*, 1968, **13**, 312-317.
- 28 R. Lide, ed., *CRC Handbook of Chemistry and physics*, CRC press, Boca Raton, 1996.
- 29 H. Toghiani, R. K. Toghiani and D. S. Viswanath, *J. Chem. Eng. Data*, 1994, **39**, 63-67.
- 30 V. I. Anisimov, *Zhurn. Fiz. Khimii*, 1953, **27**, 264.
- 31 I. C. Hubbard, *Z. Phys. Chem.*, 1910, **74**, 207.
- 32 S. E. Wood, S. Langer and K. Battino, *J. Chem. Phys.*, 1960, **32**, 1389-1393.
- 33 I. Cibulka, V. Hynek, R. Holub and J. Pick, *Collect. Czech. Chem. C.*, 1979, **44**, 295-306.